Pressure-Induced Confined Metal from the Mott Insulator $Sr_3Ir_2O_7$

Yang Ding,[1,2,3,*] Liuxiang Yang,[1,3] Cheng-Chien Chen,[2,4] Heung-Sik Kim,[5] Myung Joon Han,[5] Wei Luo,[6] Zhenxing Feng,[7] Mary Upton,[2] Diego Casa,[2] Jungho Kim,[2] Thomas Gog,[2] Zhidan Zeng,[1,3] Gang Cao,[8] Ho-kwang Mao,[1,3,9] and Michel van Veenendaal[2,10]

[1]*Center for High Pressure Science and Technology Advanced Research, Pudong, Shanghai 201203, China*
[2]*Advanced Photon Source, Argonne National Laboratory, Argonne, Illinois 60439, USA*
[3]*HPSynC, Geophysical Laboratory, Carnegie Institution of Washington, Argonne, Illinois 60439, USA*
[4]*Department of Physics, University of Alabama at Birmingham, Birmingham, Alabama 35294, USA*
[5]*Department of Physics, Korea Advanced Institute of Science and Technology, Daejeon 305-701, Republic of Korea*
[6]*Condensed Matter Theory Group, Department of Physics, Box 530, SE-751 21 Uppsala, Sweden*
[7]*Chemical Sciences and Engineering, Argonne National Laboratory, Argonne, Illinois 60439, USA*
[8]*Department of Physics and Astronomy, University of Kentucky, Lexington, Kentucky 40506, USA*
[9]*Geophysical Laboratory, Carnegie Institution of Washington, Washington, D.C. 20015, USA*
[10]*Department of Physics, Northern Illinois University, De Kalb, Illinois 60115, USA*

(Received 28 October 2015; revised manuscript received 29 January 2016; published 24 May 2016)

The spin-orbit Mott insulator $Sr_3Ir_2O_7$ provides a fascinating playground to explore insulator-metal transition driven by intertwined charge, spin, and lattice degrees of freedom. Here, we report high-pressure electric resistance and resonant inelastic x-ray scattering measurements on single-crystal $Sr_3Ir_2O_7$ up to 63–65 GPa at 300 K. The material becomes a confined metal at 59.5 GPa, showing metallicity in the *ab* plane but an insulating behavior along the *c* axis. Such an unusual phenomenon resembles the strange metal phase in cuprate superconductors. Since there is no sign of the collapse of spin-orbit or Coulomb interactions in x-ray measurements, this novel insulator-metal transition is potentially driven by a first-order structural change at nearby pressures. Our discovery points to a new approach for synthesizing functional materials.

DOI: 10.1103/PhysRevLett.116.216402

The $5d$ transition-metal oxides have recently attracted tremendous interest because the interplay between spin-orbit (SO) interaction and electron correlation in these materials can lead to novel states of matter, such as quantum spin liquids, topological orders, and potentially high-temperature superconductors [1–5]. Among these compounds, the Ruddlesden-Popper series of iridates $Sr_{n+1}Ir_nO_{3n+1}$ (where n is the number of $SrIrO_3$ perovskite layers between extra SrO layers) has been extensively studied. In these systems, the nearly cubic crystal field splits the $5d$ shell into the e_g and t_{2g} levels leading to a ${t^5}_{2g}$ configuration for Ir^{4+}. The strong spin-orbit interaction further splits the t_{2g} orbitals into $J_{\text{eff}} = 1/2$ and $3/2$ states (where J_{eff} is effective total angular momentum). The singly occupied $J_{\text{eff}} = 1/2$ state can be further split by the electron-electron Coulomb repulsion, giving rise to Mott insulating behavior [6,7]. With their correlated spin, charge, and lattice responses to external perturbation, perovskite iridates provide a fascinating system for studying the competition and cooperation of fundamental interactions.

The double-layered perovskite $Sr_3Ir_2O_7$ [8] appears in a unique position in this series [4,8–15]. Its structure has been regarded to be tetragonal ($I4/mmm$, with $a = 3.9026$ Å and $c = 20.9300$ Å [16,17]), but other studies also reveal that the crystal symmetry could be orthorhombic ($Bbcb$, with $a = 5.522$ Å, $b = 5.521$ Å, and $c = 20.917$ Å [18]) or even monoclinic ($C2/c$, with $a = 5.5185$ Å, $b = 5.5099$ Å, and $c = 20.935$ Å [19]). The charge gap of $Sr_3Ir_2O_7$ (~0.1–0.3 eV) is comparable to the magnitude of the underlying exchange interaction [20–22], and such an insulating state is considered in the weak Mott limit. Small perturbations, such as carrier doping, magnetic field, or external pressure, can affect the stability of the insulating phase. Therefore, this system provides a valuable platform for exploring the collapse of the Mott gap. Indeed, in addition to a dimensionality-driven insulator-metal transition (IMT) in the iridate Ruddlesden-Popper series [23], recent experiments have found that a small amount of La substitution for Sr in $(Sr_{1-x}La_x)_3Ir_2O_7$ can melt away its insulating gap and lead to a correlated metallic state [24], showing that the system resides in close proximity to an IMT phase boundary.

Conventional wisdom dictates that pressure has a similar effect as carrier doping. However, to date, high-pressure studies on $Sr_3Ir_2O_7$ have been inconclusive due to the lack of consistent experimental results. Li *et al.* claimed that $Sr_3Ir_2O_7$ undergoes an IMT-like transition at ~13 GPa [25], but Zocco *et al.* found that the insulating state persists up to 104 GPa [12]. In addition, whereas Zhao *et al.*

reported a second-order structure transition at ~15 GPa, Donnerer *et al.* only discovered a first-order structure transition at ~54 GPa [17]. Based on first-principle calculations, Donnerer *et al.* also predicted an IMT concurring with the structural change [17]. Further experiments are thereby necessary to clarify these ambiguities.

In this Letter, we present electric resistance and resonant inelastic x-ray scattering (RIXS) [26] measurements for the first time on single-crystal $Sr_3Ir_2O_7$ in a diamond anvil cell (DAC) at pressures up to ~63–65 GPa at 300 K. The resistance measurements indicate that an IMT is present at ~59.5 GPa, with the high-pressure phase exhibiting a novel confinement phenomenon: a metallic behavior within the *ab* plane but an insulating one along the *c* axis. This intriguing phenomenon is reminiscent of the strange metal phase in cuprate superconductors [27,28]. Because the RIXS measurement shows robust spin-orbit and electron Coulomb interactions within the investigated pressure range, this novel IMT is potentially driven by a first-order structure change at a nearby pressure as reported by recent diffraction measurements [17].

Figure 1 shows the electric resistance measurements on a $Sr_3Ir_2O_7$ single crystal at different pressures. In this experiment, resistances within the *ab* plane R_{ab} [Fig. 1(a)] and along the *c* axis R_c [Fig. 1(b)] are measured at the same time for each pressure point with the standard four-probe-electrode-circuit method [29]. Further experimental details are given in Supplemental Material [30]. At low pressures (18.4 and 43.15 GPa), the system is an insulator, with its

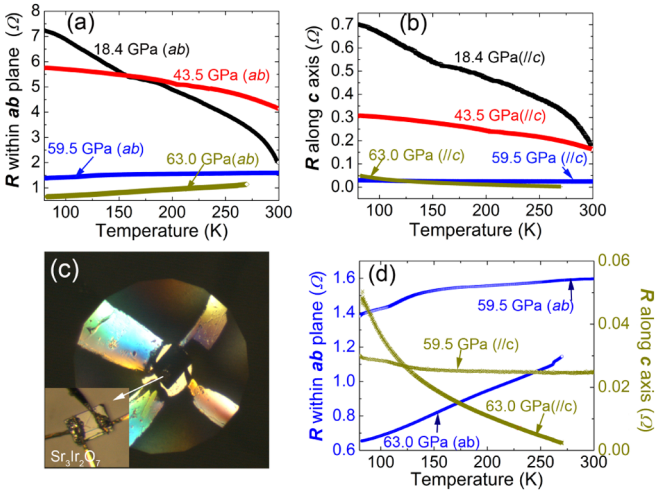

FIG. 1. Electric resistance measurements of single-crystal $Sr_3Ir_2O_7$ at high pressure (a) within the *ab* plane and (b) along the crystal *c* axis. (c) Four gold electric leads and single-crsytal $Sr_3Ir_2O_7$ loaded into a symmetric diamond anvil cell. The inset shows two of the leads attached to the top of the single crystal, and the other two attached to the bottom. Each diamond culet is approximately 300 μm wide. (d) Temperature dependences of the resistances at 59.5 and 63.0 GPa. The system shows metallic behavior in the *ab* plane, whereas it still exhibits an insulating state along the *c* axis.

resistances increasing with decreasing temperature ($dR_{ab}/dT < 0$ and $dR_c/dT < 0$). However, at 59.5 and 63.0 GPa [Fig. 1(d)], the material shows a clear metallic behavior within the *ab* plane ($dR_{ab}/dT > 0$) and an insulatinglike state along the *c* axis ($dR_c/dT < 0$). Such behavior is highly unusual. Although the resistivity ratio between the *ab* plane and *c* axis could differ by several orders of magnitude for an anisotropic metal, localization in only one direction rarely occurs. This novel "confinement" phenomenon is reminiscent of the strange metal phase in overdoped cuprate superconductors [27,28]. Together with the recent discovery of Fermi-arc features in Sr_2IrO_4, the similarity between the high-pressure phase of $Sr_3Ir_2O_7$ and the cuprates shows the potential promise of superconductivity in perovskite iridates $Sr_{n+1}Ir_nO_{3n+1}$ [35,36]. To the best of our knowledge, this is the first time that a confined metal has been found at high pressure. Our discovery thereby points to a new way of synthesizing novel states of matter.

IMTs in correlated transition-metal oxides could be driven by bandwidth broadening, structural transition, or the collapse of electron-electron interaction [37,38]. Furthermore, the insulating state in $Sr_3Ir_2O_7$ is associated with a strong spin-orbit interaction, another parameter that can trigger an IMT. An understanding of the mechanism underlying the pressured-induced IMT in $Sr_3Ir_2O_7$ requires detailed knowledge of the pressure evolution of the electronic structure. However, such information was unattainable until our recent integration of the RIXS and DAC techniques [39].

Figure 2 displays the high-pressure Ir L_3-edge RIXS data collected with a scattering vector along the $[0, \pi/b, 0]$ (indexed by a pesudotetragonal symmetry for simplicity) direction in a horizontal scattering geometry. In the high-pressure experiments, the $Sr_3Ir_2O_7$ single crystal is loaded with neon gas as the pressure medium in a Mao-type symmetric DAC. Based on diffraction measurements [17], the unit cell of $Sr_3Ir_2O_7$ has been compressed by nearly 6% at 64.6 GPa. Accordingly, from 0.98 to 64.8 GPa, the scattering vector q spans from $[0, \pi, 0]$ at 0.98 GPa, $[0, 0.99\pi, 0]$ at 12.4 GPa, $[0, 0.96\pi, 0]$ at 23.6 GPa, $[0, 0.95\pi, 0]$ at 34.4 GPa, and $[0, 0.94\pi, 0]$ at 43.8 GPa, due to a sample size reduction with pressure (see Supplemental Material for further details [30]). In addition to the zero-energy quasielastic peak (indicated as *A*), three other major peaks in the RIXS map [Fig. 2(a)] were identified at an energy loss of 0.25 (*B*), 0.64 (*C*), and 2.5 (*D*) eV. The resonant energy for peak *D* is 11.218 KeV, and the resonant energy for *C* and *B* is 11.216 KeV.

Previous RIXS studies [40–43] have identified peak *D* as a crystal-field (CF) excitation between the Ir 5*d* t_{2g} and e_g orbitals, possibly mixed with a small amount (5%) of charge-transfer excitation from the oxygen 2*p* ligands [44]. In a nearly cubic crystal field, peak *C* is the spin-orbit exciton related to transition between the $J_{\text{eff}} = 1/2$ and 3/2

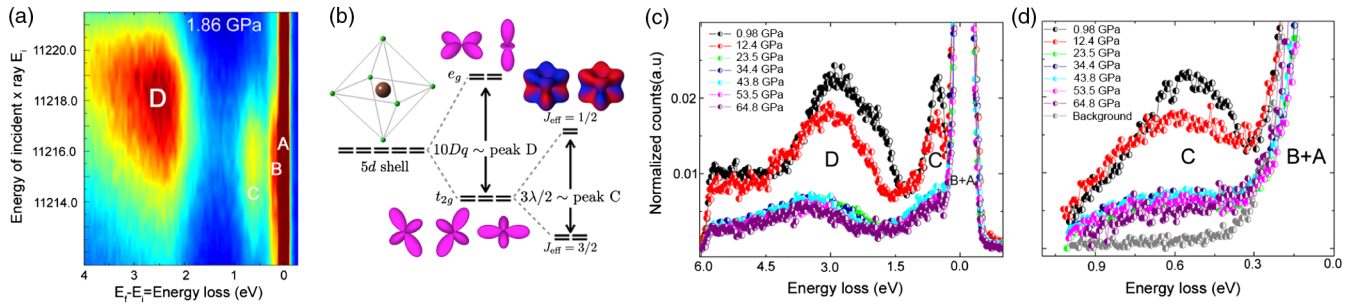

FIG. 2. (a) Ir L_3-edge RIXS map collected at 1.86 GPa. (b) Atomic energy-level diagram for an Ir^{4+} ion in an octahedral crystal field. (c) and (d) RIXS data collected at high pressures between an energy loss of −1.0 and 6.0 eV, and between 0.0 and 1.0 eV, respectively. The incident energy is 11.216 KeV.

states [35,41,45]. In other iridate compounds, a noncubic splitting of $J_{\text{eff}} = 1/2$ was also observed [35,42,43,46]. In the low-energy region (<0.3 eV), peak B has been previously attributed to excitations of magnetic origin [47–50], which may overlap with phonon excitations of the DAC and the sample. No significant change is observed in the low-energy area of peaks A and B during our measurements.

To more accurately obtain the energy loss and linewidth of peaks C and D, a peak-fitting analysis is performed. The results are shown in Figs. 3(a) and 3(b), as well as in Table I. Figure 3 displays two significant changes in peak D: First, whereas its excitation energy grows with applied pressure, it is only weakly pressure dependent above 53.5 GPa [Fig. 3(a)]. Second, the linewidth drops significantly above 53.5 GPa [Fig. 3(b)]. In comparison, the energy of peak C increases with pressure up to 23.6 GPa, then decreases. Above 53.5 GPa, peak C's energy is increased by ∼15% compared to that at ambient condition [Fig. 3(a)]. Overall, the linewidth of peak C is increased by pressure, but significantly reduced above 53.5 GPa. Although a tetragonal splitting could increase the linewidth of peak C, this change also should have been found in peak D [this change is anticipated in peak D as well but is not observed, as shown in Fig. 3(b)]; yet Fig. 3(b) does not show such a change. Therefore, the different pressure dependence between peak D and peak C below 53.5 GPa could imply that a weak dispersion of spin-orbiton excitation exists in the low-pressure phase, despite the fact that the excitation has a predominant intrasite character [45,46]. In RIXS measurements of Sr_2IrO_4, the dispersive behavior of spin-orbiton excitation is also more obvious than the crystal-field excitation [40]. Above 53.5 GPa, the pressure dependence of peak C and peak D becomes more complicated.

As the line widths of peaks C and D both drop above 53.5 GPa when the ab plane of $Sr_3Ir_2O_7$ becomes metallic, a correlation appears between the linewidth reduction and the IMT. Because the IrO_6 octahedron symmetry becomes even lower above 54 GPa [17], the linewidth reduction cannot arise from the tetragonal splitting. In contrast, a self-energy correction due to electron interaction could contribute to the intrinsic lifetime broadening. Therefore, the sudden drop of the linewidth for both peaks C and D could indicate that the effective Coulomb repulsion U is slightly weakened in the high-pressure metallic phase due to enhanced screening. Nonetheless, because the bandwidth broadening and lattice changes are expected to be more substantial, the small reduction of effective U should be regarded as a consequence, instead of a cause of the pressure-induced IMT.

In addition, the RIXS results unambiguously show that spin-orbit coupling strength λ (equal to two thirds the energy of peak C) is robust up to 64.8 GPa, where the system already becomes metallic according to our resistance measurements. Therefore, the pressure-induced IMT

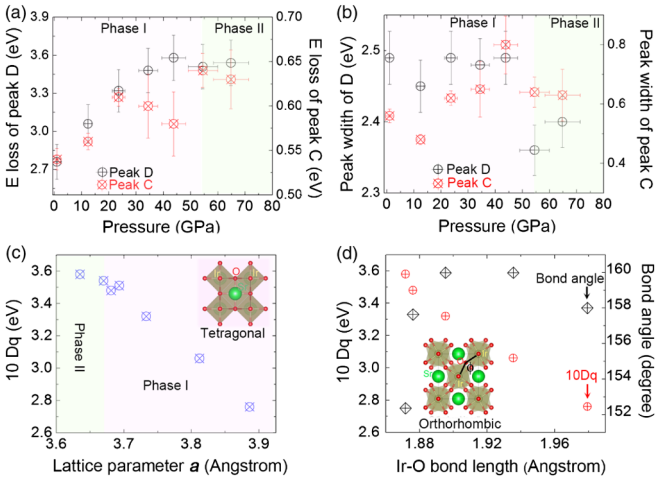

FIG. 3. (a) Energies of crystal-field excitation $10Dq$ measured from peak D and the spin-orbit exciton peak C in RIXS as a function of pressure. (b) Pressure dependences of the RIXS spectral line widths of peaks D and C. (c) Crystal-field excitation energy $10Dq$ versus the lattice parameter a from diffraction measurements. Areas of different color represent phases with different structures. (d) The fitted ab plane Ir-O bond length and the Ir-O-Ir bond angle. The inset displays the orthorhombic structure of $Sr_3Ir_2O_7$ viewed along the c axis in the low-pressure, insulating phase.

TABLE I. The position and width (FWHM) of the CF excitation peak C and the SO exciton peak D obtained from peak-fitting analysis. The lattice parameter in the high-pressure monoclinic phase is averaged over the a and b axes. Here P stands for pressure.

P (GPa)	a (Å)	$10Dq$ (eV)	Width (CF)	SO exciton (eV)	Width (SO)
0.98	3.8860	2.76	2.49	0.54	0.56
12.40	3.8120	3.06	2.45	0.56	0.48
23.60	3.7330	3.32	2.49	0.61	0.62
34.40	3.6810	3.48	2.48	0.60	0.65
43.80	3.6350	3.58	2.49	0.58	0.80
53.50	3.6931	3.51	2.36	0.64	0.64
64.80	3.6699	3.54	2.40	0.63	0.63

in $Sr_3Ir_2O_7$ cannot be driven by a collapse of the spin-orbit interaction. We also note that although the L_2/L_3-edge branching ratio in x-ray absorption spectroscopy could be used to obtain the ground state expectation value of $\langle \mathbf{L} \cdot \mathbf{S} \rangle$, the λ value alone cannot be determined in this manner [51,52].

We now discuss further implications of our RIXS data by comparing them to diffraction measurements. If the energy loss of peak D is approximated as the crystal-field splitting $10Dq$ in a perfect O_h symmetry, we can examine whether the relationship $10Dq = K/d^n_{\text{Ir-O}}$ $(n = 3.5 - 7)$ is still valid under pressure, where K is a constant and $d_{\text{Ir-O}}$ is the Ir-O bond length. However, Fig. 3(c) shows that $10Dq$ (represented by peak D's energy loss) and the effective Ir-O bond length (represented by the lattice parameter a) no longer comply with the relation $10Dq = K/d^n_{\text{Ir-O}}$ $(n = 3.5 - 7)$. This result suggests that the ab plane Ir-O-Ir bond angle ϕ must be taken into account [53,54]. In this case, the symmetry of $Sr_3Ir_2O_7$ in the low-pressure, insulating state cannot be effectively treated as $I4/mmm$ [16,17]. This conclusion is supported by earlier measurements that determined the crystal symmetry of $Sr_3Ir_2O_7$ as orthorhombic (space group $Bbca$) [18,25] or even monoclinic (space group $C2/c$) [12] with ϕ equal to 158° at ambient conditions.

By using ϕ and n as variation parameters, we obtained the Ir-O bond length and bond angle using $10Dq = K/d^n_{\text{Ir-O}}$ (with details given in Supplemental Material [30]). The results are plotted in Fig. 3(d) and listed in Table II. The best fit is obtained for $n = 4.6$, which is comparable to the results in other $5d$ transition-metal oxides [55]. Figure 3(d) shows that the bond angle ϕ decreases when the system is approaching the metallic phase below the critical pressure, thereby leading to an increased rotation of the IrO_6 octahedron with respect to the c axis. In fact, such a conclusion remains qualitatively valid for all $n = 3.5 - 7$ in the fitting. Such a pressure-induced octahedron rotation could provide a dehybridization mechanism that prevents the system from becoming metallic [56,57] at pressures below 50 GPa.

TABLE II. The fitted ab plane Ir-O bond length $d_{\text{Ir-O}}$ and bond angle ϕ based on $10Dq = K/d^n_{\text{Ir-O}}$.

	P (GPa)	a Å	$10Dq$ (eV)	ϕ	$d_{\text{Ir-O}}$
$n = \mathbf{4.6}$	0.98	3.886	2.76	158	1.9794
	12.4	3.812	3.06	159.98	1.9355
	23.6	3.733	3.32	159.98	1.8954
	34.4	3.681	3.48	157.64	1.8761
	43.8	3.635	3.58	152.36	1.8717

As a first-order approximation, the pervoskite structure tolerance factor [58], $t = (R_{\text{Sr}} + R_{\text{O}}/\sqrt{2}(R_{\text{Ir}} + R_{\text{O}}))$ (where R_{Sr}, R_{O}, and R_{Ir} represent the atomic radii of Sr, O, and Ir, respectively), can be used to gauge the stability of structure. When the rotation angle is considered, the tolerance factor t is proportional to $1/\sin(\phi/2)$. Based on our fitting results, t reaches 1.02–1.04 when the rotation angle becomes less than 152° at the critical pressure of 54 GPa as reported by diffraction measurements. This value reaches the $t = 1.04$ perovskite stability limit [59]. Therefore, the structural transition above 54 GPa is likely triggered by a saturated IrO_6 octahedron rotation. The first-order structural change in turn could drive the pressure-induced insulator-metal transition in $Sr_3Ir_2O_7$, since there are no apparent changes in the electron Coulomb repulsion and spin-orbit interactions up to 65 GPa as revealed by our RIXS measurements.

Finally, since the critical pressure (53.5 GPa) in RIXS measurements is nearly identical to the structural transition pressure (54 GPa) in diffraction measurements [17], we believe that the electronic and structural transitions are likely to occur at a nearby pressure, or even concur at the same pressure point. The difference between the structural transition pressure and the insulator-metal transition pressure (59.5 GPa) determined from our transport measurements is 5.5 GPa. This mismatch is potentially caused by nonhyrostaticity of the silicon oil and the coarse pressure step size. We also note that previous transport measurements on powder samples may suffer from uncertainties possibly due to the existence of grain boundaries. Moreover, our single-crystal measurements do not show any abrupt change in the pressure range below 50 GPa, thereby excluding the existence of a structural phase transition below this pressure point, which is consistent with the more recent diffraction measurement by Donnerer *et al.* [17].

To conclude, our findings have unraveled a nontrivial interplay between the structural and electronic properties in $Sr_3Ir_2O_7$, and even more generally in the Ruddlesden-Popper series of iridates, where various material families also exhibit correlated spin, charge, and lattice degrees of freedom. Our discovery of a novel high-pressure metallic phase with an intriguing confinement phenomenon similar to that found in overdoped cuprate superconductors

suggests that superconductivity could potentially be found in doped $Sr_3Ir_2O_7$ under high pressure. Moreover, pressure shows a distinct effect compared to doping or dimensionality change, thereby pointing to a new way of synthesizing novel states of matter that are inaccessible with other methods.

The authors acknowledge useful discussions with Elizabeth Nowadnick. The RIXS measurements are performed at sectors 30 ID-B and 27 ID-B of Advanced Photon Source, a U.S. Department of Energy (DOE) Office of Science user facility operated by Argonne National Laboratory (ANL) supported by the U.S. DOE Award No. DE-AC02-06CH11357. C. C. C. is supported by the Aneesur Rahman Postdoctoral Fellowship at ANL. H.-S. K. and M. J. H. were supported by the Basic Science Research Program through NRF (Grant No. 2014R1A1A2057202) and by Samsung Advanced Institute of Technology (SAIT). G. C. acknowledges NSF support via Grant No. DMR1265162. H.-k. M. acknowledges the support of DOE-BES under Award No. DE-FG02-99ER45775 and NSFC Grant No. U1530402. M. v. V. is supported by the U.S. DOE under Award No. DE-FG02-03ER46097, and by the Institute for Nanoscience, Engineering, and Technology at Northern Illinois University.

*yang.ding@hpstar.ac.cn

[1] G. Jackeli and G. Khaliullin, Phys. Rev. Lett. **102**, 017205 (2009).
[2] W. Witczak-Krempa, G. Chen, Y. B. Kim, and L. Balents, Annu. Rev. Condens. Matter Phys. **5**, 57 (2014).
[3] F. Wang and T. Senthil, Phys. Rev. Lett. **106**, 136402 (2011).
[4] A. Biswas, K.-S. Kim, and Y. H. Jeong, arXiv:1508.04929.
[5] J. G. Rau, E. K.-H. Lee, and H.-Y. Kee, arXiv:1507.06323.
[6] B. J. Kim, H. Ohsumi, T. Komesu, S. Sakai, T. Morita, H. Takagi, and T. Arima, Science **323**, 1329 (2009).
[7] B. Kim *et al.*, Phys. Rev. Lett. **101**, 076402 (2008).
[8] S. Moon *et al.*, Phys. Rev. Lett. **101**, 226402 (2008).
[9] J.-M. Carter, V. Vijay Shankar, and H.-Y. Kee, Phys. Rev. B **88**, 035111 (2013).
[10] Q. Wang, Y. Cao, J. A. Waugh, S. R. Park, T. F. Qi, O. B. Korneta, G. Cao, and D. S. Dessau, Phys. Rev. B **87**, 245109 (2013).
[11] Y. Okada *et al.*, Nat. Mater. **12**, 707 (2013).
[12] D. A. Zocco, J. J. Hamlin, B. D. White, B. J. Kim, J. R. Jeffries, S. T. Weir, Y. K. Vohra, J. W. Allen, and M. B. Maple, J. Phys. Condens. Matter **26**, 255603 (2014).
[13] P. D. C. King *et al.*, Phys. Rev. B **87**, 241106 (2013).
[14] L. Moreschini *et al.*, Phys. Rev. B **89**, 201114 (2014).
[15] B. M. Wojek, M. H. Berntsen, S. Boseggia, A. T. Boothroyd, D. Prabhakaran, D. F. McMorrow, H. M. Ronnow, J. Chang, and O. Tjernberg, J. Phys. Condens. Matter **24**, 415602 (2012).
[16] Z. Zhao *et al.*, J. Phys. Condens. Matter **26**, 215402 (2014).
[17] C. Donnerer *et al.*, Phys. Rev. B (to be published).
[18] H. Matsuhata, I. Nagai, Y. Yoshida, S. Hara, S.-i. Ikeda, and N. Shirakawa, J. Solid State Chem. **177**, 3776 (2004).
[19] T. Hogan, L. Bjaalie, L. Zhao, C. Belvin, X. Wang, C. G. Van de Walle, D. Hsieh, and S. D. Wilson, arXiv:1603.07390v1.
[20] S. Boseggia, R. Springell, H. C. Walker, A. T. Boothroyd, D. Prabhakaran, D. Wermeille, L. Bouchenoire, S. P. Collins, and D. F. McMorrow, Phys. Rev. B **85**, 184432 (2012).
[21] M. M. Sala, S. Boseggia, D. F. McMorrow, and G. Monaco, Phys. Rev. Lett. **112**, 026403 (2014).
[22] S. Fujiyama, K. Ohashi, H. Ohsumi, K. Sugimoto, T. Takayama, T. Komesu, M. Takata, T. Arima, and H. Takagi, Phys. Rev. B **86**, 174414 (2012).
[23] H. Zhang, K. Haule, and D. Vanderbilt, Phys. Rev. Lett. **111**, 246402 (2013).
[24] T. Hogan *et al.*, Phys. Rev. Lett. **114**, 257203 (2015).
[25] L. Li, P. P. Kong, T. F. Qi, C. Q. Jin, S. J. Yuan, L. E. DeLong, P. Schlottmann, and G. Cao, Phys. Rev. B **87**, 235127 (2013).
[26] L. J. P. Ament, M. van Veenendaal, T. P. Devereaux, J. P. Hill, and J. van den Brink, Rev. Mod. Phys. **83**, 705 (2011).
[27] P. W. Anderson, Science **256**, 1526 (1992).
[28] S. L. Cooper and K. E. Gray, *Anisotropy and Interlayer Coupling in the High Tc Cuprates*, Physical Properties of High-Temperature Superconductors IV (World Scientific, Singapore, 1994).
[29] K. Shimizu, K. Suhara, M. Ikumo, M. I. Eremets, and K. Amaya, Nature (London) **393**, 767 (1998).
[30] See Supplemental Material at http://link.aps.org/supplemental/10.1103/PhysRevLett.116.216402, which includes Refs. [31–34], for detailed information on experimental settings, methods, and partial data analysis.
[31] G. Cao, Y. Xin, C. Alexander, J. Crow, P. Schlottmann, M. Crawford, R. Harlow, and W. Marshall, Phys. Rev. B **66**, 214412 (2002).
[32] T. Gog, D. M. Casa, A. H. Said, M. H. Upton, J. Kim, I. Kuzmenko, X. Huang, and R. Khachatryan, J. Synchrotron Radiat. **20**, 74 (2013).
[33] Y. V. Shvyd'ko *et al.*, J. Electron Spectrosc. Relat. Phenom. **188**, 140 (2013).
[34] M. G. Brik, J. Phys. Chem. Solids **68**, 1341 (2007).
[35] J. Kim *et al.*, Phys. Rev. Lett. **108**, 177003 (2012).
[36] Y. K. Kim, O. Krupin, J. D. Denlinger, A. Bostwick, E. Rotenberg, Q. Zhao, J. F. Mitchell, J. W. Allen, and B. J. Kim, Science **345**, 187 (2014).
[37] M. Imada, i. A. Fujimor, and Y. Tokura, Rev. Mod. Phys. **70**, 1039 (1998).
[38] Y. Ding *et al.*, Phys. Rev. Lett. **112**, 056401 (2014).
[39] Y. Ding, J. Fernandez-Rodriguez, J. Kim, F. Li, D. Casa, M. Upton, T. Gog, H.-k. Mao, and M. van Veenendaal, Phys. Rev. B **86**, 094107 (2012).
[40] K. Ishii, I. Jarrige, M. Yoshida, K. Ikeuchi, J. Mizuki, K. Ohashi, T. Takayama, J. Matsuno, and H. Takagi, Phys. Rev. B **83**, 115121 (2011).
[41] J. Kim, M. Daghofer, A. H. Said, T. Gog, J. van den Brink, G. Khaliullin, and B. J. Kim, Nature (London) **5**, 4453 (2014).
[42] H. Gretarsson *et al.*, Phys. Rev. Lett. **110**, 076402 (2013).
[43] X. Liu *et al.*, Phys. Rev. Lett. **109**, 157401 (2012).

[44] V. M. Katukuri, H. Stoll, J. van den Brink, and L. Hozoi, Phys. Rev. B **85**, 220402 (2012).
[45] B. H. Kim, G. Khaliullin, and B. I. Min, Phys. Rev. Lett. **109**, 167205 (2012).
[46] M. M. Sala, K. Ohgushi, A. Al-Zein, Y. Hirata, G. Monaco, and M. Krisch, Phys. Rev. Lett. **112**, 176402 (2014).
[47] C. Dhital *et al.*, Phys. Rev. B **86**, 100401 (2012).
[48] J.-i. Igarashi and T. Nagao, Phys. Rev. B **89**, 064410 (2014).
[49] M. Moretti Sala *et al.*, Phys. Rev. B **92**, 024405 (2015).
[50] J. Kim, A. H. Said, D. Casa, M. H. Upton, T. Gog, M. Daghofer, G. Jackeli, J. van den Brink, G. Khaliullin, and B. J. Kim, Phys. Rev. Lett. **109**, 157402 (2012).
[51] D. Haskel, G. Fabbris, M. Zhernenkov, P. P. Kong, C. Q. Jin, G. Cao, and M. van Veenendaal, Phys. Rev. Lett. **109**, 027204 (2012).
[52] J. P. Clancy, N. Chen, C. Y. Kim, W. F. Chen, K. W. Plumb, B. C. Jeon, T. W. Noh, and Y.-J. Kim, Phys. Rev. B **86**, 195131 (2012).
[53] K. H. Kim, H. S. Kim, and M. J. Han, J. Phys. Condens. Matter **26**, 185501 (2014).
[54] A. Lupascu *et al.*, Phys. Rev. Lett. **112**, 147201 (2014).
[55] M. G. Brik, J. Phys. Chem. Solids **68**, 1341 (2007).
[56] S. J. Moon, H. Jin, W. S. Choi, J. S. Lee, S. S. A. Seo, J. Yu, G. Cao, T. W. Noh, and Y. S. Lee, Phys. Rev. B **80**, 195110 (2009).
[57] M. Ge, T. F. Qi, O. B. Korneta, D. E. D. Long, P. Schlottmann, W. P. Crummett, and G. Cao, Phys. Rev. B **84**, 100402(R) (2011).
[58] S. Helmut Kronmller, M. Johnsson, and P. Lemmens, *Handbook of Magnetism and Advanced Magnetic Materials* (John Wiley & Sons, New York, 2007).
[59] A. F. Sammells and M. V. Mundschau, *Nonporous Inorganic Membranes: For Chemical Processing* (Wiley-VCH, Germany, 2006).